Tip-Enhanced Raman Chemical and Chemical Reaction Imaging in H_2O with Sub-3 nm Spatial Resolution

Patrick Z. El-Khoury*

Physical Sciences Division, Pacific Northwest National Laboratory, P.O. Box 999, Richland, WA 99352, USA

ABSTRACT: Reproducible chemical and chemical reaction nano-imaging at solid-liquid interfaces remains challenging, particularly when resolutions on the order of a few nm are sought after. In this work, we demonstrate the latter through liquid tip-enhanced Raman (TER) measurements that target gold nanoplates functionalized with 4-mercaptobenzonitrile (MBN). In addition to chemical imaging and local optical field nano-visualization with high spatial resolution, we observe the signatures of 4-mercaptobenzoic acid, which forms as a result of plasmon-induced hydrolysis of MBN. Evidently, the solvent leads to distinct plasmon-induced/enhanced chemical reaction pathways that have not been documented. This work shows that such reactions that take place at solid-liquid interfaces can be tracked with a record sub-3 nm spatial resolution via TER spectral nano-imaging in liquids.

Imaging and identifying the chemical constituents of heterogeneous interfaces with molecular resolution is important to diverse areas of study, including heterogenous (photo)catalysis, investigations of microbial communication pathways, and testing emerging nanophotonic device architectures, to name a few. Interfacial chemical nano-imaging is possible through the combination of scanning probe microscopy (herein atomic force microscopy, AFM) and optical spectroscopy (herein Raman scattering).[1,2] More generally, both linear and nonlinear spectral nano-imaging has been demonstrated in measurements targeting increasingly complex analytes.[3] From single molecules isolated under ultrahigh vacuum at ultralow temperatures,[3,4] through molecular assemblies on plasmonic metals and nanostructures,[5] to molecular and material systems in solution,[7] established and emerging tools of nano-optics and nanophotonics continue to contribute to an increased fundamental understanding of interfaces.

As elegantly summarized in a recent review article,[7] tip-enhanced Raman (TER) scattering is ideally suited for the investigation of chemistry at solid-liquid interfaces. Indeed, from the pioneering work of Zenobi and co-workers[8] to our group's own investigation of chemical transformations at the solid-liquid interface,[9] the promise of liquid TER spectral nano-imaging is unwavering.[7] That said, there are several outstanding issues that need to be addressed in the area of liquid TER imaging. First, robust and reproducible measurements are scarce, in part because of the technical difficulties of such measurements. Second, the spatial resolution of TER measurements of solid liquid interfaces is limited to ~10 nm,[10,11] and even to 10's of nm in the case of AFM-based liquid TER mapping.[12,13] Third, the role of the solvent not only on local chemistry, but also on the local optical fields remains poorly understood, beyond a general appreciation of plasmon resonance shifts in distinct dielectric media. In this work, some of these open questions are addressed through TER measurements that characterize 4-mercaptobenzonitrile (MBN)-functionalized gold nanoplates in solution.

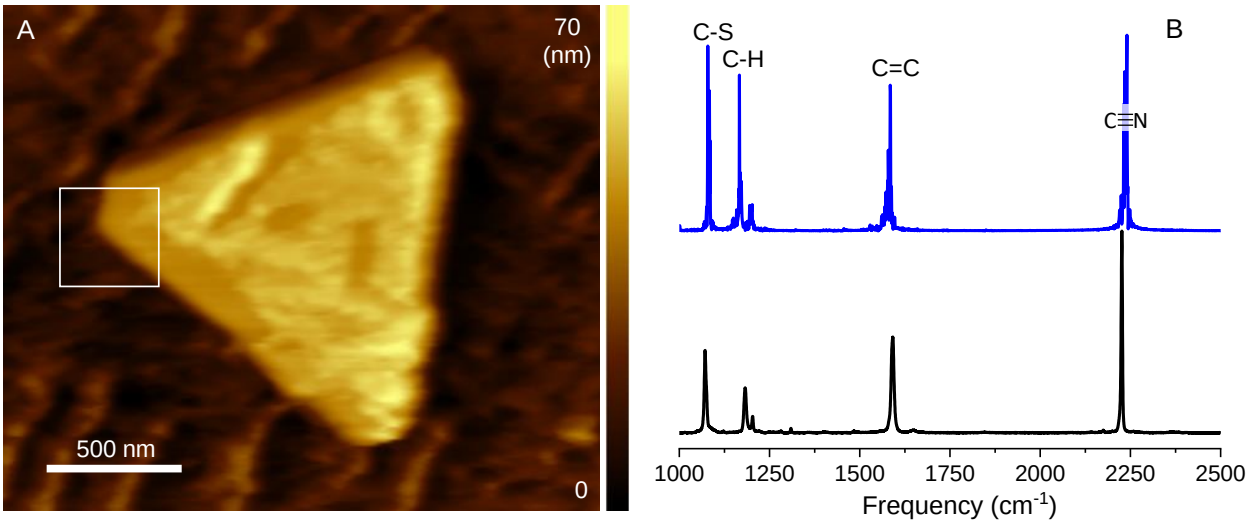

Figure 1. A topographic AFM image of an MBN functionalized 60 nm thick triangular gold nanoplatelet in H_20 is shown in A. The white triangular area is further analyzed via TER below. Panel B compares an experimental Raman spectrum of solid MBN (lower black trace) to a theoretical spectrum (upper blue trace) computed through ab initio molecular dynamics simulations (see reference 14). The principle resonances are marked by the bonds to which the majority of amplitude is localized at the distinct frequencies.

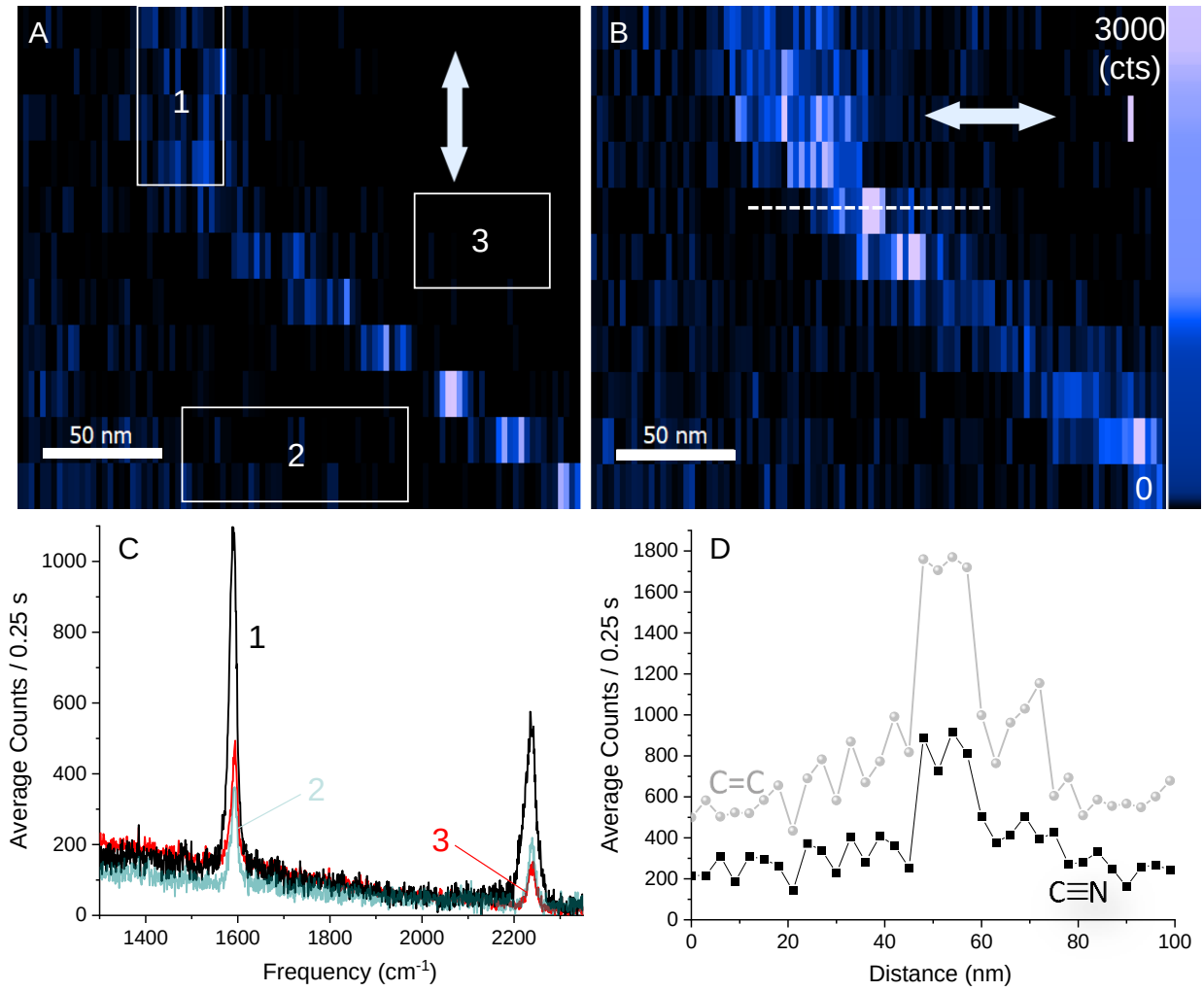

Figure 2. High spatial resolution bottom excitation/collection TER maps of the area highlighted using a white square in Figure 1A. Panels A and B (integrated, 1580-1600 cm^{-1}) were recorded using the in-plane polarization directions indicated in the insets using light blue double-sided arrows. Spatial averaging of the response in regions 1, 2 and 3 in panel A results in the spectra plotted in panel C. Cross-sectional line cuts along the red line in panel B results in the spectrally-averaged traces in panel D. In D, the spectra were integrated over a spectral window of 20 cm^{-1} centered at the two resonances.

An MBN-coated triangular gold nanoplate in H_20 is visualized using AFM in Figure 1A. Heterogenous surface coverage is visible atop the plate, with minimal (apparent) molecular coverage towards its left apex and lower left edge. The measurements and analyses that follow are focused to the areas that feature lower molecular coverage. For reference, Figure 1B additionally shows experimental and theoretical Raman spectra of MBN.[14] In decreasing order of energy, the four modes highlighted using short notation are the nitrile stretching, aromatic C=C stretching, aromatic C-H stretching, and C-S stretching vibrations of MBN. We will mostly rely on the nitrile (2237 cm^{-1}) and aromatic C=C (1593 cm^{-1}) stretching vibrations in the ensuing analysis. The reader is otherwise referred to prior studies for more detailed spectral assignments.[14]

Bottom excitation/collection TER images of the white rectangular area highlighted in Figure 1A are shown in Figure 2A and 2B. The two images were sequentially recorded using distinct incident polarizations that are schematically illustrated in the insets. Besides minor intensity differences that may be associated with molecular dynamics under ambient conditions and otherwise some drifting, both maps trace the edges of the gold plates. This is consistent with several prior TER measurements of chemically functionalized gold plates, irrespective of the medium in which the measurements were performed, i.e., air vs liquid.[9,12,15] Namely, both experimental spectral nano-images as well as numerical simulations of the field profiles in the TER geometry illustrate that the signals are optimally enhanced when the probe is closely positioned near the edges of the gold plates. Here, the contrast we observe when the tip is positioned toward the edge vs off the gold structure is immediately noticeable in Figure 2C. Using the nitrile resonance of MBN as a gauge, we can deduce a ~5X near-field to far-field contrast on average. Notably, this value is vibrational resonance-dependent because of the selective enhancement of various modes, as a result of TER selection rules that differ

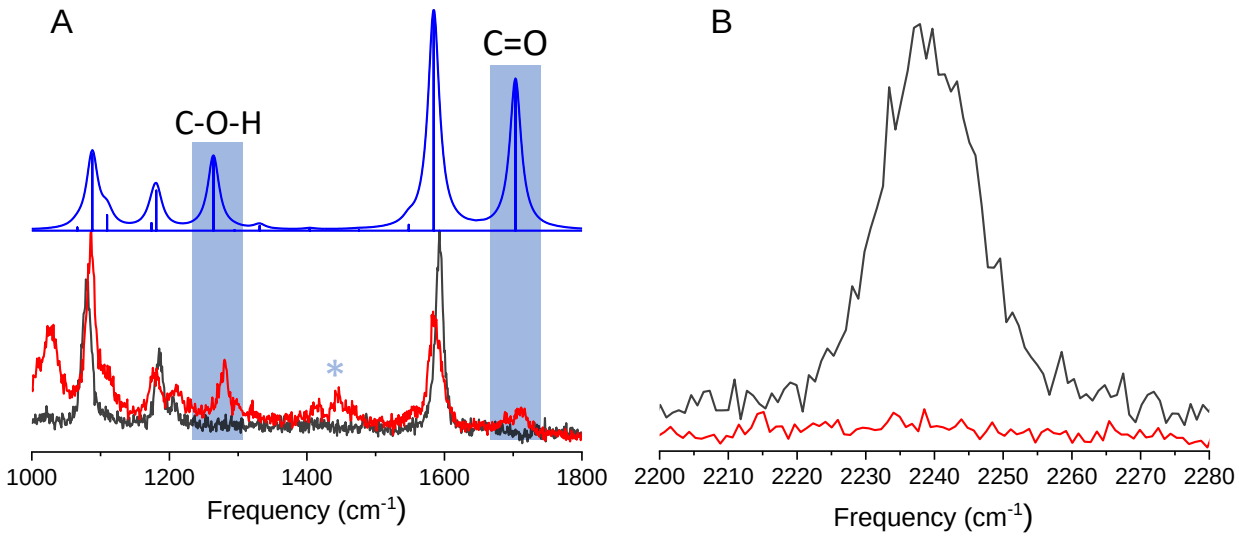

Figure 3. Spatially-averaged TER spectra containing either only MBN (black spectrum) or MBN+MBA resonances (red spectrum) are compared to a static theoretical Raman spectrum of MBA (pbe/def2-TZVP, water described using the PCM model). Resonances that involve the carboxyl group of MBA are highlighted using blue vertical rectangles. The peak at ~1400 cm^{-1} is discussed further in the main text.

from their far-field analogues.[6] At ~1590 cm^{-1} toward the resonance maximum of the aromatic C=C vibration, the observed contrast is ~3.5. This can be deduced from the spectrally-averaged TER cross-sectional line cut shown in Figure 2D. The same plot can also be used to gauge the attainable spatial resolution of our measurements: pixel-limited rise in signal in < 3 nm. To the best of our knowledge, this is the record spatial resolution for liquid TER measurements. As the local fields vary rather slowly in space around the edges of the nanoplates,[12] the fine spatial resolution documented in this study tracks sparse and otherwise non-uniform molecular coverage.

The brightest TER spectra that trace the edges of the gold plate (see Figure 2) can almost entirely be assigned to MBN,[10] with some exceptions. Namely, we observe a dozen or so spectra that contain several peaks that appear in tandem and that can be uniquely assigned to 4-mercaptobenzonic acid (MBA). Besides reasonable agreement between experiment and theory in Figure 3A and the concurrent disappearance of the nitrile signature in Figure 3B, two prior TER investigations of MBA add confidence to our assignment.[15,16] Indeed, both our group[15] and others[16] have observed broad resonances in the 1350-1450 cm^{-1} (marked with an asterisk in the lower part of Figure 3A) that have been associated with a distinct binding geometry of MBA, wherein the CO_2 moiety interacts strongly with the underlying metal. The indexed C=O and C-O-H resonances in Figure 3A otherwise arise from MBA molecules that are chemically bound to the metal through the sulphur atom.[15] This seems to be well-captured by the theoretical model used here, which takes water implicitly into account using a polarizable continuum model.

The observation of the hydrolysis product reveals that the solvent is not merely a medium, but rather a reactant in our case of plasmon-assisted hydrolysis as probed via TER spectral imaging. This is contrasted with the case of MBN interrogated at the solid-air interface, where no degradation was observable under nearly identical experimental (ambient) conditions, barring the presence of water.[6,17] The present results may also be used to comment on (some) aspects of the local optical fields that are encountered in TER at the solid-air vs solid-liquid interface. Besides the fact that the images track the magnitudes of local optical fields in the TER geometry,[6,17] the observation of a single symmetric nitrile resonance in Figure 3B suggests the absence of optical rectification in this work *vs* in TER spectral imaging at solid-air interfaces.[17] Since optical rectification has been associated with the onset of tunnelling plasmons,[18-21] the results in Figure 3B in turn suggest that quantum plasmons may not be operative under our current experimental conditions. This may result from effects as mundane as tuned resonances in air *vs* water, or may hint at a more complex mechanism, the origin of which requires exhaustive simulations that account for the molecules, solvent, and plasmonic metal. Such simulations that lie at the interface between classical and quantum regimes are not possible at present.

On a technical note, the measurements described here still require bottom access to the sample (see the supporting information section), and also a plasmonic substrate for optimal signal enhancement using in-plane polarized excitation. More general TER in solution requires further developments and optimization. Besides generalizing the herein-described approach using different (non)linear optical spectroscopies in combination with AFM in solution, split excitation-collection (e.g., side excitation-bottom collection) is potentially promising toward more general TERS in liquids.[4] This premise will be tested in follow-on work.

In conclusion, we demonstrate record spatial resolution (< 3 nm) and rapid chemical reaction nano-imaging (0.25 s/pixel) in solution using TER spectroscopy. We find that

the solvent affects both local chemistry and the local optical fields in non-standard ways that have not been described to date. Besides leading to novel chemical reaction pathways, the solvent appears to alter the local plasmonic response in ways that are not fully understood. Further work is needed to account for some of our observations, necessitating further theory developments at the interface between classical and quantum theories.

ASSOCIATED CONTENT

Supporting Information. Coarse AFM-TERS maps of the nanotriangle analyzed in the main text, micro-Raman images of the tip showing our fine alignment procedure, a collection of TERS spectra of the parent and product, additional medium resolution TERS maps of the right edge of the triangular plate shown in Figure 1, and experimental details.

AUTHOR INFORMATION

Corresponding Author

*patrick.elkhoury@pnnl.gov

Funding Sources

U.S. Department of Energy, Office of Science, Basic Energy Sciences, Chemical Sciences, Geosciences, and Biosciences Division, Condensed Phase and Interfacial Molecular Science program, FWP 16248.
Laboratory Directed Research and Development program at Pacific Northwest National Laboratory, through the Chemical Dynamics Initiative.

ACKNOWLEDGMENT

The author acknowledges support from the U.S. Department of Energy, Office of Science, Basic Energy Sciences, Chemical Sciences, Geosciences, and Biosciences Division, Condensed Phase and Interfacial Molecular Science program, FWP 16248. Some of the measurements that are described in this work were performed using equipment that was partially developed using funding from the Laboratory Directed Research and Development program at Pacific Northwest National Laboratory, through the Chemical Dynamics Initiative.

REFERENCES

(1) Stockle, R. M.; Suh, Y. D.; Deckert V.; Zenobi, R. Nanoscale Chemical Analysis by Tip-Enhanced Raman Spectroscopy. *Chem. Phys. Lett.* **2000**, *318*, 131-136. DOI: 10.1016/S0009-2614(99)01451-7

(2) Pettinger, B.; Schambach, P.; Villagomez, C. J.; Scott, N. Tip-Enhanced Raman Spectroscopy: Near-Fields Acting on a Few Molecules. *Annu. Rev. Phys. Chem.* **2012**, *63*, 379-399. DOI: 10.1146/annurev-physchem-032511-143807

(3) Mahapatra, S.; Li, L. F.; Schultz J. F.; Jiang, N. Tip-Enhanced Raman Spectroscopy: Chemical Analysis with Nanoscale to Angstrom Scale Resolution. *J. Chem. Phys.* **2020**, *153,* 010902. DOI: 10.1063/5.0009766

(4) Wang, C. F.; El-Khoury, P. Z. Multimodal (Non)Linear Optical NanoImaging and NanoSpectroscopy. *J. Phys. Chem. Lett.* **2022**, *13*, 7350-7354. DOI: 10.1021/acs.jpclett.2c01993

(5) Lee, J.; Crampton, K. T.; Tallarida, N.; Apkarian, V. A. Visualizing Vibrational Normal Modes of a Single Molecule with Atomically Confined Light. *Nature* **2019**, *568*, 78-82. DOI: 10.1038/s41586-019-1059-9

(6) El-Khoury, P. Z. Tip-Enhanced Raman Scattering on Both Sides of the Schrödinger Equation. *Acc. Chem. Res.* **2021**, *54*, 4576-1583. DOI: 10.1021/acs.accounts.1c00597

(7) Britz-Grell, A. B.; Saumer, M.; Tarasov, A. Challenges and Opportunities of Tip-Enhanced Raman Spectroscopy in Liquids. *J. Phys. Chem. C* **2021**, *125*, 21321-21340. DOI: 10.1021/acs.jpcc.1c05353

(8) Schmid, T.; Yeo, B. -S.; Leong, G.; Stadler, J.; Zenobi, R. Performing Tip-Enhanced Raman Spectroscopy in Liquids. *J. Raman Spec.* **2009**, *40*, 1392-1399. DOI: 10.1002/jrs.2387

(9) Bhattarai, A.; El-Khoury, P. Z. Tip-Enhanced Chemical Reaction Imaging at the Solid-Liquid Interface *via* TERS. *J. Phys. Chem. Lett.* **2019**, *10*, 2817-2822. DOI: 10.1021/acs.jpclett.9b00935

(10) Pfisterer, J. H. K.; Baghernejad, M.; Giuzio, G.; Domke, K. F. Reactive Mapping of Nanoscale Defect Chemistry Under Electrochemical Reaction Conditions. *Nat. Commun.* **2019**, *10*, 5702. DOI: 10.1038/s41467-019-13692-3

(11) Touzalin, T.; Joiret, S.; Lucas, I. T.; Maisonhaute, E. *Electrochem. Commun.* **2019**, *108*, 106557. DOI: 10.1016/j.elecom.2019.106557

(12) Bhattarai, A.; Joly, A. G.; Krayev, A.; El-Khoury, P. Z. Taking the Plunge: Nanoscale Chemical Imaging of Functionalized Gold Triangles in H_20 *via* TERS. *J. Phys. Chem. C* **2019**, *123*, 7376-7380. DOI: 10.1021/acs.jpcc.9b00867

(13) Kumar, N.; Su, W.; Vesely, M.; Weckhuysen, B. M.; Pollard, A. J.; Wain, A. J. Nanoscale Chemical Imaging of Solid-Liquid Interfaces Using Tip-Ehanced Raman Spectroscopy. *Nanoscale* **2018**, *10*, 1815-1824. DOI: 10.1039/C7NR08257F

(14) Aprà, E.; Bhattarai, A.; Baxter, E.; Wang, S.; Johnson, G. E.; Govind, N.; El-Khoury, P. Z. *Appl. Spectrosc.* **2020**, *74*, 1350. DOI: 10.1177/0003702820923392

(15) Li, Z.; Kurouski, D. Elucidation of Photocatalytic Properties of Gold-Platinum Bimetallic Nanoplates Using Tip-Nehcned Raman Spectroscopy. *J. Phys. Chem. C* **2020**, *124*, 12850-12854. DOI: 10.1021/acs.jpcc.0c04274

(16) Gabel, M.; O'Callahan, B. T.; Groome, C.; Wang, C. -F.; Ragan, R.; Gu, Y.; El-Khoury, P. Z. Mapping Molecular Adsorption Configurations with < 5 nm Spatial Resolution through Ambient Tip-Enhanced Raman Imaging. *J. Phys. Chem. Lett.* **2021**, *12*, 3586-3590. DOI: 10.1021/acs.jpclett.1c00661

(17) Li, Z.; Kurouski, D. Tip-Enhanced Raman Analysis of Plasmonic and Photocatalytic Properties of Copper Nanomaterials. *J. Phys. Chem. Lett.* **2021**, *12*, 8335-8340. DOI: 10.1021/acs.jpclett.1c02500

(18) El-Khoury, P. Z.; Schultz, Z. D. From SERS to TERS and Beyond: Molecules as Probes of Nanoscopic Optical Fields *J. Phys. Chem. C* **2020**, *50*, 27267-27275. DOI: 10.1021/acs.jpcc.0c08337

(19) Wang, C. -F.; O'Callahan, B. T.; Kurouski, D.; Krayev, A; Schultz, Z. D.; El-Khoury, P. Z. Suppressing Molecular Charging, Nanochemistry, and Optical Rectification in the Tip-Enhanced Raman Geometry. *J. Phys. Chem. Lett.* **2020**, *11*, 5890-5895. DOI: 10.1021/acs.jpclett.0c01413

(20) Kos, D.; Assumpcao, D. R.; Guo, C.; Baumberg, J. J. Quantum Tunneling Induced Optical Rectification and Plasmon-Enhanced Photocurrent in Nanocavity Molecular Junctions. *ACS Nano* **2021**, *15*, 14535-14543. DOI: 10.1021/acsnano.1c04100

(21) Wang, H.; Yao, K.; Parkhill, J. A.; Schultz, Z. D. Detection of Electron Tunneling Across Plasmonic Nanoparticle-Film Junctions Using Nitrile Vibrations. *Phys. Chem. Chem. Phys.* **2018**, *19*, 5786-5786. DOI: https://doi.org/10.1039/C6CP08168A